



Catalytic arene alkylation over H-Beta zeolite: Influence of zeolite shape selectivity and reactant nucleophilicity

Xin Zeng^a, Zichun Wang^{a,b,*}, Jia Ding^a, Leizhi Wang^a, Yijiao Jiang^b, Catherine Stampfl^c, Michael Hunger^d, Jun Huang^{a,*}

^a Laboratory for Catalysis Engineering, School of Chemical and Biomolecular Engineering & Sydney Nano Institute, The University of Sydney, NSW 2006, Australia

^b Department of Engineering, Macquarie University, Sydney, New South Wales 2109, Australia

^c School of Physics & Sydney Nano Institute, The University of Sydney, Sydney, New South Wales 2006, Australia

^d Institute of Chemical Technology, University of Stuttgart, 70550 Stuttgart, Germany

ARTICLE INFO

Article history:

Received 6 May 2019

Revised 21 September 2019

Accepted 23 September 2019

Keywords:

Beta zeolite

Benzylation reaction

Shape selectivity

Reactant nucleophilicity

Solid-state NMR spectroscopy

ABSTRACT

Renewable arenes and aromatic alcohols can be derived from lignocellulose by biorefineries, which has been considered as a sustainable alternative to replace petrochemical feedstocks in the synthesis of monobenzylation products, key industrial intermediates, via benzylation reactions. Zeolites with micropores are the most widely used catalysts in the benzylation of arenes, however, their performance suffers from diffusion limitations in converting large arenes. In this work, mesoporous and microporous H-Beta zeolites were prepared and applied in the systematic study of benzylation of arenes (benzene, toluene, *p*-xylene and mesitylene) with benzyl alcohol (BA). The porous structure of these zeolites has been confirmed by XRD, BET and TEM techniques. The catalytically active Brønsted acid sites (BAS) were determined by quantitative ¹H magic-angle spinning (MAS) nuclear magnetic resonance (NMR) experiments. The benzylation studies have shown that introducing mesopores into H-Beta zeolites can significantly increase the diffusion/access of arenes to surface sites, particularly for bulky arenes (e.g. mesitylene), while micropores are mainly selective for the conversion of small arenes (e.g. benzene). Increasing the nucleophilicity of arenes with more alkyl groups can enhance their catalytic performance in mesopores, however, the increase hinders their conversion in micropores because of the shape selectivity due to their increasing molecular size. Compared to mesopores, micropores promote the conversion of small arenes (e.g. benzene), which can be additionally enhanced by a high Brønsted acidity. Therefore, introducing a suitable porosity balanced with acidity are keys in the tailoring of the catalytic performance of H-Beta zeolites for target benzylation reactions.

© 2019 Elsevier Inc. All rights reserved.

1. Introduction

Non-edible lignocellulose biomass is regarded as a renewable and environmentally friendly alternative to fossil fuels in the production of energy and valuable chemicals [1,2]. Lignocellulose consists of cellulose, hemicellulose, and lignin. Cellulose and hemicellulose are polymers of glucose and monosaccharides, respectively, and have been widely utilized in biorefineries around the world. Lignin is composed of disordered polymerized phenylpropane monomers via hydroxyl or methoxy substituents, which is interesting as a renewable raw feedstock for bio-derived

aromatics. Recently, various arenes and aromatic alcohols have been derived from lignocellulose biomass [3–5]. The conversion of these bio-derived aromatic compounds has high potential for the sustainable production of aromatic-containing chemicals, and can fit into current chemical processes.

Benzylated arenes are key industrial intermediates and building blocks in the production of petrochemicals, pharmaceuticals, fine chemicals, and polymers [6]. These compounds can be derived from the benzylation of arenes with benzyl alcohol (BA) or benzyl chloride, which are typical acid-catalysed Friedel–Crafts alkylation reactions [7,8]. Lewis acidic halides (e.g. AlCl₃, FeCl₃, InCl₃, BF₃) and protic acids (e.g. H₂SO₄, HCl, HNO₃) are most frequently used in the synthesis of benzylated arenes [8], however, they cause severe environmental issues and problems with catalyst separation and regeneration [9]. Environmentally friendly heterogeneous catalysts have been developed to replace homogeneous acids, including

* Corresponding authors at: Laboratory for Catalysis Engineering, School of Chemical and Biomolecular Engineering & Sydney Nano Institute, The University of Sydney, NSW 2006, Australia (J. Huang, Z. Wang).

E-mail addresses: zichun.wang@mq.edu.au (Z. Wang), jun.huang@sydney.edu.au (J. Huang).

zeolites and mesoporous silica-alumina [7,10–22], acidic oxides and sulphides [23–30], and heteropoly acids (HPAs) [15,31].

Zeolites, having crystalline framework, high surface area, regular porous structure, and strong acidity, are the most popular catalysts used in current chemical processes [10]. Brønsted acid sites (BAS) on zeolites, which are protons compensating the negatively charged, tetrahedrally coordinated Al atoms substituting Si atoms in the zeolite framework, are active sites for benzylation reactions [7,11–13]. The suitable micropores (<2 nm) and strong acidity of zeolites can remarkably promote the formation of diphenylmethane with a high selectivity in comparison to other catalysts [7,11,14,15]. However, microporous zeolites often suffer from diffusion limitations, poor selectivity, and a strong shortening of the catalyst lifetime for bulky substrates [16].

Introducing mesopores (2–50 nm in diameter) or hierarchical pore architectures offer promising solutions to facilitate molecule transportation and improve the catalytic performance of zeolites in the benzylation [16–20]. The application of hierarchical architectures of H-ZSM-5 zeolites in the benzylation of mesitylene with benzyl chloride has been reported to increase the reaction rate k for over 65 times compared to microporous H-ZSM-5 zeolites [19]. Improving the catalytic performance of zeolites by increasing the mesoporosity is also observed on mesoporous mordenite in alkylation reactions [32,33]. In the catalytic benzylation of naphthalene with benzyl chloride, mesoporous H-Beta (H β) zeolites afford a benzyl chloride conversion of 90–100%, much higher than the conversion of ca. 25% obtained with microporous H β zeolites [20].

In general, benzylation of arenes is proceeded by replacing a hydrogen atom of the aromatic ring with a benzyl group from a benzylating agent in the presence of a catalyst [8]. Zeolites having strong Brønsted acidity can facilitate the formation of benzyl cations (C₆H₅CH₂⁺), which then attack the aromatic ring for an electrophilic substitution [34]. Alkyl groups as nucleophilic reagents can contribute via electron donation effects when bounded to aromatic rings. Therefore, more substituted methyl groups on the aromatic ring is often considered to promote benzylation reactions with a higher catalytic performance [6]. However, the shape selectivity of zeolites limits the diffusion and access of aromatics with more alkyl groups, i.e. reducing their catalytic performance [11,21].

In this work, we provide a systematic study on the influence of acidity and pore size of microporous zeolites and the reactant nucleophilicity effects on the catalytic benzylation over H β zeolites, since H β zeolites are highly active and selective to monobenzylation products compared to other zeolites (e.g. H-Y, H-ZSM-5 and mordenite) [7,11–13,21,22]. H β zeolites with different Si/Al ratios and micro- and mesopores have been successfully synthesized for the benzylation of arenes (benzene, toluene, p-xylene and mesitylene) with benzyl alcohol. Benzyl alcohol is a kind of environmentally friendly alkylating agent to replace benzyl chloride for green chemical processes, producing water rather than stoichiometric hydrochloride. Compared to benzyl chloride, the application of benzyl alcohol often suffers from fast self-condensation to generate dibenzyl ether (DBE), but is limited by the further conversion of DBE with arenes [35], leading to a low selectivity to monobenzylation products.

2. Experimental Section

2.1. Catalyst preparation

All chemicals were purchased in analytical standard without further purification, including silica sol (30 wt% SiO₂ suspension in H₂O, Sigma-Aldrich), tetraethyl ammonium hydroxide aqueous solution (35 wt% TEAOH in water, Sigma-Aldrich), sodium aluminate

(50–56% Al₂O₃, 37–45% Na₂O, Sigma-Aldrich), sodium hydroxide (NaOH, reagent grade, ≥98%, pellets (anhydrous), Sigma-Aldrich), aluminum sulfate (98% Al₂(SO₄)₃·18 H₂O, Sigma-Aldrich), fumed silica (Sigma-Aldrich, 395 m²/g).

As described earlier [34], microporous Na-Beta zeolites (Na β) were prepared by dissolving sodium aluminate in an aqueous solution of TEAOH. Then, NaOH and silica sol were added to the mixture under vigorous stirring for half hour. Afterwards, the gels with molar composition of Na₂O: (TEA)₂O:H₂O:SiO₂:Al₂O₃: = 5.1:12.5:1300:62: x , where x is adjusted to the desired Si/Al ratio, were transferred to a Teflon lined stainless autoclave. The mixture was kept at 413 K for 4 days for crystal growth under static conditions. The solid products were collected by centrifugation, filtration, washing and drying at 353 K for 12 h. Finally, the solid products were transferred to quartz crucibles and calcined in air at 823 K for 2 h.

Mesoporous Na β zeolites were prepared as described earlier [36]. In brief, a mixture of NaOH (0.066 g), Al₂(SO₄)₃·18 H₂O (x g), and aqueous TEAOH (6 g) was stirred until clear, where x is adjusted to the desired Si/Al ratio. Then, fumed silica (2.0 g) was added, and the mixture was further stirred for another 1 h. The resulting gel was dried by heating at 333 K. The dry precursor lumps were ground and transferred into a 4 mL Teflon cup, which was placed into a 20 mL Teflon liner. Then, 0.3 mL of water was added into the liner without contacting the dry gel. The Teflon set was transferred into a 20 mL autoclave, which was subsequently heated at 453 K for 3 days. The resulting gel was recovered by washing, filtrating, and drying, followed by calcination in air at 823 K for 6 h.

Ammonia exchange of the obtained Na β zeolites for obtaining H β zeolites was employed as described in our earlier work [37]. Briefly, the Na β zeolites were mixed with a certain amount of 0.1 M NH₄NO₃ aqueous solution and stirred at 353 K for 3 h. After filtration and washing with deionized water till no nitrate ions could be detected, the obtained products were dried at room temperature overnight. The above procedure was repeated for four times to ensure an ion-exchange degree of >99% in the final H β zeolites. The nomenclature of H β zeolites is defined as Micro-H β - x and Meso-H β - x , for microporous and mesoporous H β zeolites, respectively, where x is assigned to 1 and 2 for samples with different Si/Al ratios listed in Table 1.

2.2. Catalyst characterization

Nitrogen adsorption-desorption measurements were performed at 77 K by an Autosorb IQ-C system to determine the specific surface areas. Before measurements, the zeolite samples were degassed at 423 K under vacuum to remove adsorbates from the surface. The specific surface areas were determined by the Brunauer–Emmett–Teller (BET) method and are summarized in Table 1.

X-ray diffraction characterization (XRD) studies was performed on a Rigaku D/Max-RB diffractometer instrument with Cu-K α (tube voltage 40 kV, tube current 100 mA, λ = 0.154 nm) radiation. The scanning angle is from 5° to 50° with a scanning rate of 2°/min were used.

Transmission electron microscopy (TEM) images were obtained by using a Philips CM120 BioFilter with samples that were mounted on a carbon-coated copper grid by drying a droplet of a suspension of the ground sample in ethanol.

The local structure and acidity of Beta zeolites were characterized by solid-state nuclear magnetic resonance (NMR) spectroscopy. For the ²⁷Al and ²⁹Si magic-angle (MAS) NMR investigations, all samples were fully hydrated at ambient temperature overnight in a desiccator containing a saturated Ca(NO₃)₂ solution. Before the ¹H and ¹³C MAS NMR experiments, the

Table 1The Si/Al ratios, surface areas, pore volumes, and average pore sizes of the H β zeolites under study.^a

Samples	Micro-H β -1	Micro-H β -2	Meso-H β -1	Meso-H β -2
Si/Al ratio	12.5	20	15	22
Specific surface areas (m ² /g)	390	404	564	597
Total pore volume (cm ³ /g)	0.34	0.33	1.02	1.11
Micropore volume (cm ³ /g)	0.26	0.27	0.20	0.19
Mesopore volume (cm ³ /g)	0.08	0.06	0.82	0.92
Pore size (NLDFT, nm)	1.1	1.2	13.5	15.7

^a Determined by Ar adsorption-desorption isotherms at 87 K. Surface areas and pore size were obtained by BET and NLDFT methods, respectively.

samples filled in glass tubes were dehydrated at 723 K for 12 h and at a pressure of less than 10^{−2} bar. These dehydrated samples were sealed in the glass tubes or directly loaded with acetonitrile-*d*₃ or acetone-2-¹³C (99.5% ¹³C-enriched, Sigma-Aldrich) using a vacuum line. Subsequently, the adsorbate-loaded samples were evacuated at room temperature for 10 min (for acetonitrile-*d*₃) or 2 h (for acetone) to remove weakly physisorbed molecules. Then, the samples were transferred into the MAS NMR rotors under dry nitrogen gas inside a glove box.

¹H, ²⁷Al, and ¹³C MAS NMR investigations were carried out on Bruker Avance III 400 WB spectrometer at resonance frequencies of 400.1, 104.3, and 100.6 MHz, respectively, with a sample spinning rate of 8 kHz using 4 mm MAS rotors. Spectra were recorded after single-pulse $\pi/2$ and $\pi/6$ excitation with repetition times of 20 s and 0.5 s for studying ¹H and ²⁷Al nuclei, respectively. Quantitative ¹H MAS NMR measurements were performed using a dehydrated H₂Na-Y zeolite (35% ion-exchanged) as an external intensity standard, which contains 58.5 mg zeolite H₂Na-Y with 1.776 mmol OH/g. ¹³C cross-polarization (CP) MAS NMR spectra were recorded with the contact time of 4 ms and the repetition time of 4 s. ²⁹Si MAS NMR experiments were performed on the same spectrometer at the resonance frequency of 79.5 MHz and with the sample spinning rate of 4 kHz using 7 mm MAS rotors. For ²⁹Si MAS NMR spectra, single-pulse $\pi/2$ excitation and high-power proton decoupling, and a recycle delay of 20 s were applied. To separate the different signals and for the quantitative evaluation of the spectra, the data were processed using the Dmfit software.

The acidity of the zeolite catalysts was also characterized by NH₃-TPD. The NH₃-TPD measurements were performed on a Chem BET TPR/TPD Chemisorption Analyzer, CBT-1, QuantaChrome instruments. Prior to the NH₃-TPD measurements, the catalyst (100 mg) was loaded and degassed at 823 K for 1 h under N₂ flow (50 mL/min) to completely remove molecules adsorbed on the samples. Then the sample was cooled to 323 K and saturated in the gas mixture of NH₃ gas (10 vol% in N₂, 25 mL/min) for 30 min, and flushed with N₂ flow (50 mL/min) for 1 h at 373 K. Ammonia desorption was carried out with increasing temperature from 373 to 873 K at a constant heating rate of 5 K/min, and the concentration of desorbed ammonia was obtained by a thermal conductivity detector connected to the TPD system.

2.3. Benzylation of arenes with benzyl alcohol

Prior to reaction, the catalyst was activated in a quartz tube under a N₂ flow of 30 mL/min at 723 K overnight, followed by cooling down to room temperature under flowing N₂ gas. A three-neck round-bottom flask (10 mL) equipped with a reflux condenser, nitrogen gas tube, and needle for the reactant injection and sample collecting were employed for the catalytic studies. The flask was purged with dry nitrogen, and subsequently, 3.5 mL of arenes (benzene, toluene, p-xylene and mesitylene) and 0.25 mL of benzyl alcohol were added and mixed in the flask. After keeping the mixture at the desired reaction temperature for 10 min under stirring, the activated catalyst (25 mg) was added into the flask, and this

time is regarded as the initial reaction time. The samples of the reaction mixture (30 μ L) were collected periodically, and subsequently filtrated and dissolved in ethanol (1 mL) for gas chromatography (GC) analysis. The reaction products were analysed by a Shimadzu GCMS-QP2010 Ultra instrument equipped with a Rtx-5 capillary column (30 m \times 0.32 mm \times 3 μ m) connected with a GC-FID detector. The benzyl alcohol conversion and product selectivity were calculated by

$$\text{Conversion } [\%] = \frac{A_{p1} + A_{p2}}{A_{p1} + A_{p2} + A_r} \times 100;$$

$$\text{Selectivity } [\%] = \frac{A_{p1} \text{ or } A_{p2}}{A_{p1} + A_{p2}} \times 100$$

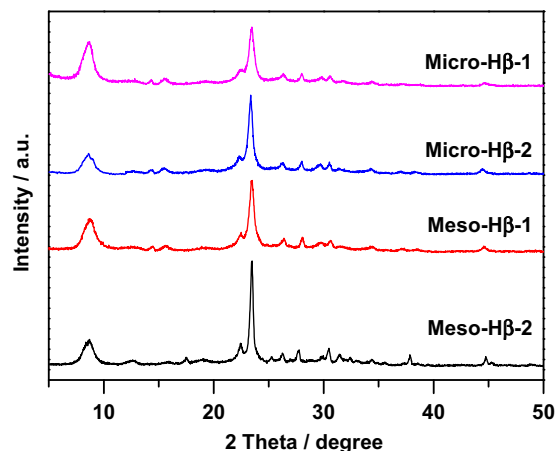
where A_{p1} and A_{p2} are the peak areas of the benzylation products obtained by GC analysis, and A_r is the peak area of benzyl alcohol.

3. Results and discussion

3.1. Physical characterization of H β Zeolites

The crystal structure of the obtained H β zeolites samples were confirmed by powder X-ray diffraction (XRD). No obvious diffraction signal of crystalline impurities could be detected. Three diffraction peaks at 2 Theta = 8.7°, 23.4° with shoulder peaks at 22.4°, and 44.5° corresponding to (1 1 0), (3 0 2), and (2 2 0) planes, respectively, were clearly observed in the obtained XRD patterns (Fig. 1), which is typical for H β zeolites with a BEA topological structure type BEA [38].

The N₂ adsorption-desorption isotherms of the H β zeolites are shown in Fig. 2. Micro-H β zeolites showed a type I isotherm typical for microporous materials according to IUPAC classification, while the Meso-H β zeolites exhibited a type VI isotherm, typically for mesoporous solids [39]. The specific surface areas and the pore

**Fig. 1.** XRD patterns of the H β zeolites under study.

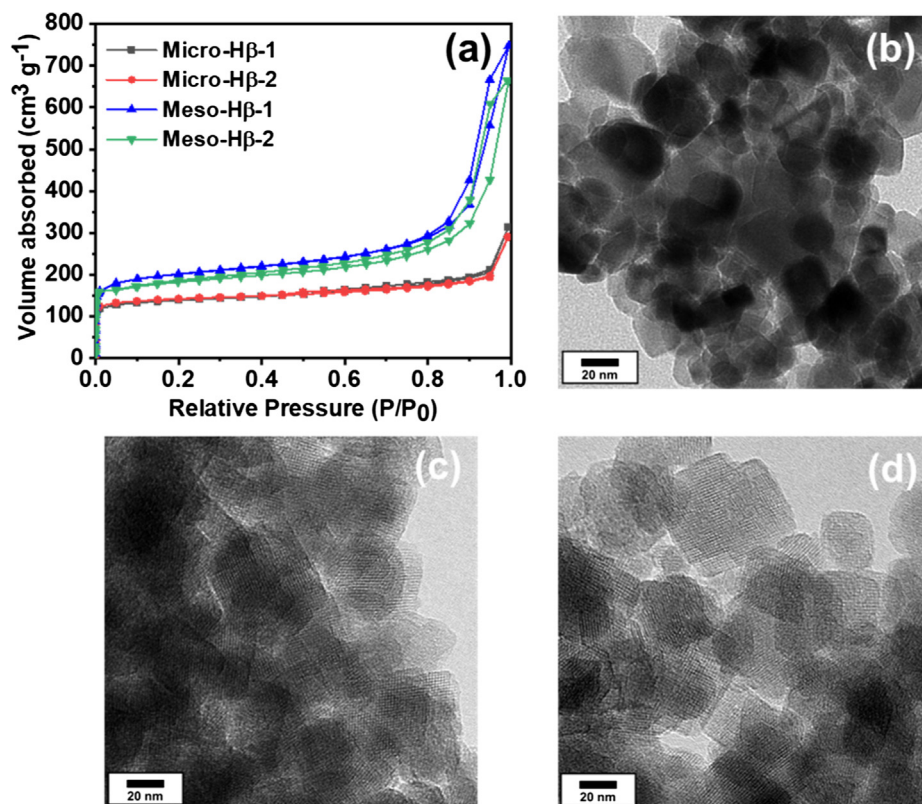


Fig. 2. Nitrogen adsorption/desorption isotherms of H β zeolites (a) and TEM images of Meso-H β -2 (b-d).

sizes are summarised in Table 1. Both the surface areas and pore sizes of the Micro-H β zeolites are similar to those reported earlier [36]. The surface areas of the Meso-H β zeolites are much larger than those of the Micro-H β zeolites, which is indicated by the strong increase of isotherms at higher relative pressures ($P/P_0 > 0.8$). The average pore diameters of the Meso-H β zeolites are in the range of 13.5–15.7 nm, i.e. 13–15 times higher than the average pore size (1.1–1.2 nm) of the Micro-H β zeolites. TEM images revealed that the Meso-H β zeolites were formed from the assembly of nanoparticles of 20–70 nm (Fig. 2b). These nanoparticles are nanosized crystals, as evidenced by lattice fringes as shown in Figs. 2c and d. The effective intergrowth of the nanosized crystals from the bulk gave rise to the substantial mesoporosity and high surface area. The obtained surface areas, pore diameters, and total pore volumes of the Meso-H β zeolites are in good agreement with a previous work [36], which indicates that both the Micro-H β and Meso-H β zeolites were successfully synthesized.

3.2. Local structure and acid sites of H β zeolites studied by ^{27}Al , ^{29}Si , ^1H , and ^{13}C NMR spectroscopy

Solid-state NMR spectroscopy was applied for the investigation of the local structure and acidity of H β zeolites, since these properties strongly influence their catalytic performance. The ^{29}Si MAS NMR spectra of H β zeolites are dominated by two strong signals at –104 ppm and –111 ppm, as shown in Fig. 3. The simulation of the ^{29}Si MAS NMR spectra required three signals at –104, –111 and –115 ppm, which were assigned to $\text{Q}^3 + \text{Si}(1\text{Al})$, $\text{Si}(\text{OAl})$, $\text{Si}(\text{OAl})$. The $\text{Si}(1\text{Al})$ and $\text{Si}(\text{OAl})$ species are ascribed to 0 or 1 Al atom located in the first coordination sphere of T-positions, for example, $\text{Si}(\text{OSi})_3\text{OAl}$. The split of the $\text{Si}(\text{OAl})$ signal is caused by two groups of different crystallographic sites [40]. Q^3 species are assigned to terminal hydroxyl groups bonded to Si atoms as

$\text{Si}(\text{OSi})_3\text{OH}$ species. The signal of which is often overlapped with the signal of $\text{Si}(1\text{Al})$ species at –104 ppm [41]. Since the formation of catalytically active BAS is accompanied by tetrahedrally coordinated Al atoms incorporated into the silica framework, the nature of Al species was further studied by ^{27}Al MAS NMR spectroscopy.

The ^{27}Al MAS NMR spectra of all H β zeolites are shown in Fig. 4. Nearly no octahedrally coordinated Al (Al^{VI}) atoms at 0 ppm, related to the extra-framework Al species (EFAl) were detected. EFAl are generally considered as the surface Lewis acid site (LAS) [42]. This indicates nearly no LAS exist in the H β zeolites under study. The dominant signal at 54 ppm was assigned to tetrahedrally coordinated Al (Al^{IV}) species. In zeolites, Al^{IV} species are introduced by the substitution of Si atoms by Al atoms in the zeolite framework [37,43], resulting in a negative charge. Hence, the ^{27}Al MAS NMR spectra shows the majority of Al atoms were incorporated into the silica framework of H β zeolites.

After ammonia exchange and calcination, the negatively charged aluminium atom can be balanced by protons, forming bridging OH groups (SiOHAl), acting as BAS in acid-catalysed reactions, such as in benzylation reactions [35,44,45]. Unlike the Brønsted acidic OH groups in amorphous silica-alumina causing ^1H MAS NMR signals, which overlap with the signals of terminal SiOH groups at 1.2–2.2 ppm [42,46,47], bridging groups in zeolites are characterized by low-field signals at chemical shifts of 3.6–5.2 ppm [42]. Therefore, the signals of BAS in zeolites can be clearly distinguished from those of non-acidic SiOH groups, and the BAS densities can be quantified via simulating the ^1H MAS NMR spectra of the dehydrated H β zeolites (Fig. 5). As shown in the simulation results of ^1H MAS NMR spectra, the signals at 1.8 ppm, and 0 and 2.4 ppm, used for the simulation, are assigned to terminal SiOH groups and AlOH groups, respectively [48]. The strong low-field signal at ca. 4.1 ppm, with a broad hump at 5.2 ppm are widely accepted as signals of bridging SiOHAl groups and disturbed bridg-

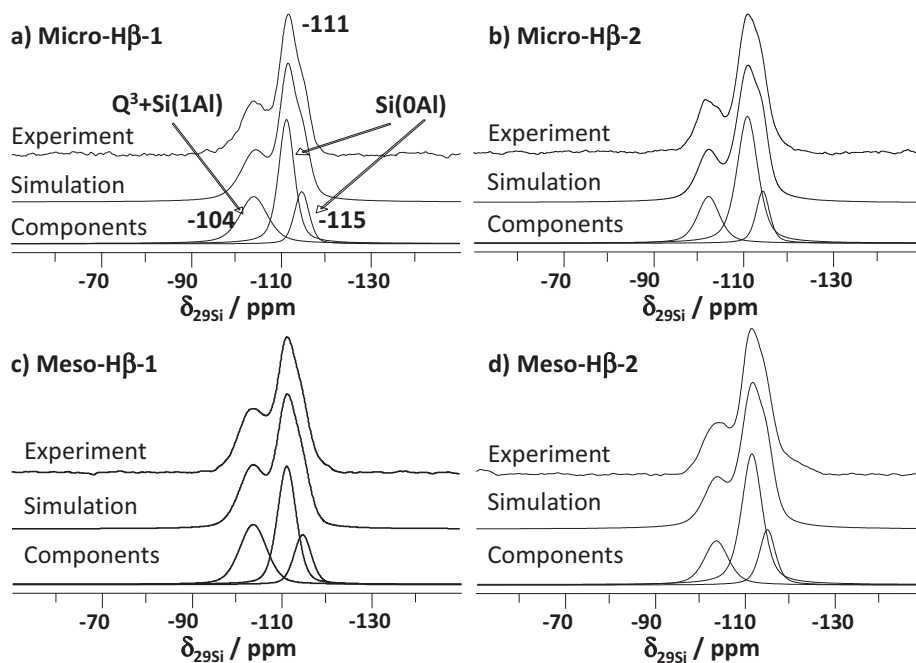


Fig. 3. ^{29}Si MAS NMR spectra of the H β zeolites under study.

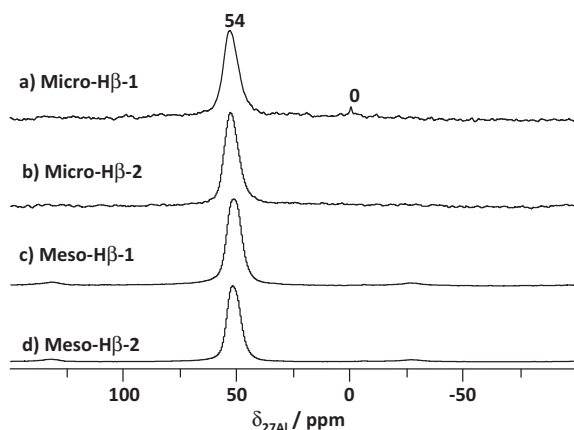


Fig. 4. ^{27}Al MAS NMR spectra of the H β zeolites under study.

ing SiOHAl groups, respectively [41,48]. Their signal intensities ($\delta_{1\text{H}} = 4.1\text{--}5.2$ ppm) were utilized to calculate the densities of BAS as summarised in Table 2. In both Micro-H β and Meso-H β zeolites, the BAS density decreases with increasing the Si/Al ratio. At a similar Si/Al ratio, Micro-H β zeolites yielded a higher BAS density than the Meso-H β zeolites counterparts, which indicates that some of the tetrahedrally coordinated Al atoms in Meso-H β zeolites incorporated into defect structures similar to those of amorphous silica-alumina.

Because of the higher electronegativity of silicon atoms in comparison with aluminium atoms, a higher Si/Al ratio affords a higher electronegativity of the framework. This higher framework electronegativity is accompanied by an increased charge withdrawal from the hydroxyl protons of the bridging OH groups, and therefore, an increase of their acid strength [49]. Upon adsorption of a weak base, e.g. acetonitrile- d_3 (CD_3CN), hydrogen bonds ($\text{O}\cdots\text{H}\cdots\text{NCD}_3$) are generated between surface OH groups and probe molecules. These hydrogen bonds can induce characteristic low-field shifts ($\Delta\delta_{1\text{H}}$) of ^1H MAS NMR signals, which correlate

with the acid strength of surface OH groups. A larger $\Delta\delta_{1\text{H}}$ means a higher strength of surface protons [42,43]. Therefore, the acid strength of surface protons can be evaluated by the adsorbate-induced low-field shift $\Delta\delta_{1\text{H}}$, e.g. occurring upon CD_3CN adsorption [46]. As shown in Fig. 6, the signal of terminal SiOH groups ($\delta_{1\text{H}} = 1.8$ ppm) was shifted to low field ($\Delta\delta_{1\text{H}} = 3.2\text{--}3.3$ ppm), which is typical for weak-acidic silanol protons. A much stronger low-field shift ($\Delta\delta_{1\text{H}} = 7.2\text{--}8$ ppm) was observed for the bridging hydroxyl protons having a much stronger acid strength than silanol protons. Notably, two kinds of bridging OH groups were probed in Fig. 5. They seem to provide a similar acid strength as reported in literature [50,51]. A similar mobility (or line shape of ^1H MAS NMR) was observed with all H β zeolites upon adsorption of CD_3CN . Therefore, the small increase of $\Delta\delta_{1\text{H}}$ of the signal centers from 7.2 to 8 ppm indicates a slight increase of the acid strength with increasing the Si/Al ratio.

The acidity of H β zeolites was also studied using NH_3 -TPD experiments. The NH_3 -TPD profile is shown in Fig. 7, and the number of BAS was summarized in Table 2. In general, a higher desorption temperature in NH_3 -TPD indicates a higher binding energies between the adsorbed ammonia molecules and the surface acid sites depends on the higher strength of acid sites [52]. Two signals at high and low temperature can be distinguished in Fig. 7, representing for two types of BAS with strong and weak strength, respectively, in H β zeolites. The total number of BAS decreased in the order of Micro-H β -1 > Micro-H β -2 > Meso-H β -1 > Meso-H β -2, well in line with the results obtained from ^1H MAS NMR experiments. Moreover, the number of both strong and weak BAS are decreased in the same order, and thus, Micro-H β zeolites possess higher Brønsted acidity compared Meso-H β zeolites.

3.3. Benzylation of arenes with benzyl alcohol

The obtained H β zeolites were utilised in the benzylation of arenes, such as benzene, toluene, *p*-xylene and mesitylene with benzyl alcohol at 353 K for 4 h. The role of the acidity and shape selectivity of the H β zeolites, and the reactant nucleophilicity and molecular size of arenes on the benzylation of BA were

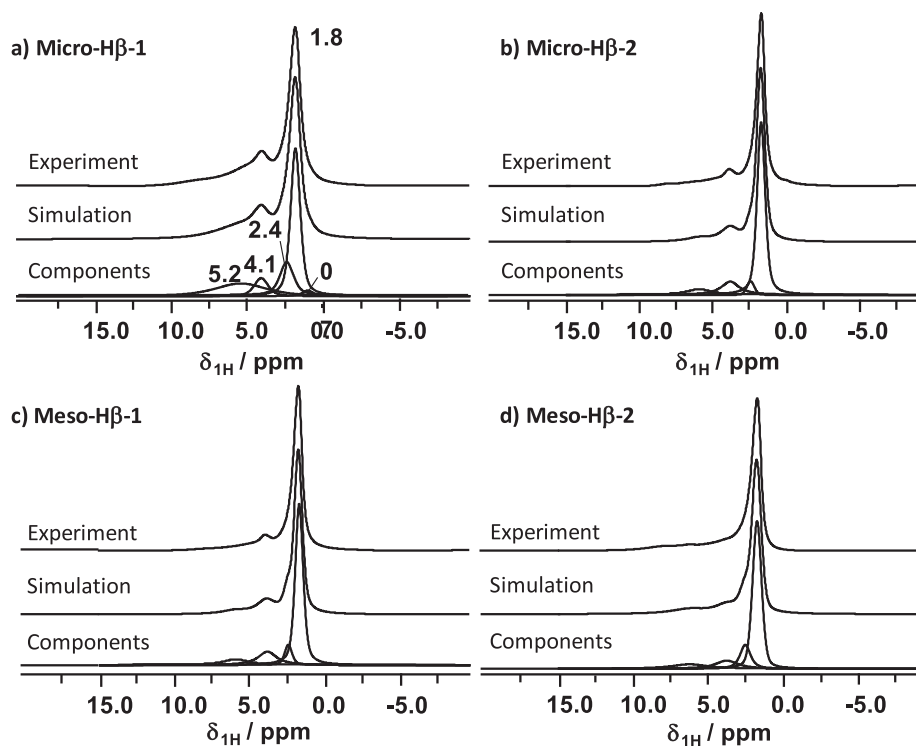


Fig. 5. ^1H MAS NMR spectra of the dehydrated H β zeolites and their simulations (bottom).

Table 2
Brønsted acid sites (BAS) of the H β zeolites under study.

Samples	Micro-H β -1	Micro-H β -2	Meso-H β -1	Meso-H β -2
BAS density (mmol/g) ^a	0.52	0.45	0.35	0.27
BAS strength ($\Delta\delta_{1\text{H}}/\text{ppm}$) ^b	7.2	7.5	7.6	8
Number of BAS (per nm ²) ^c	0.66	0.50	0.46	0.27
BAS density (mmol/g) ^d	0.58	0.42	0.21	0.14
Strong BAS (mmol/g) ^d	0.17	0.15	0.12	0.08
Weak BAS (mmol/g) ^d	0.41	0.27	0.09	0.06

^a Determined by the corresponding ^1H MAS NMR spectra.

^b Determined by ^1H MAS NMR spectra of dehydrated H β zeolites loaded with CD_3CN as shown in Fig. 6.

^c Calculated by $(\text{BAS density} \times \text{Avogadro constant})/(\text{specific surface area})$.

^d Determined by NH_3 -TPD experiments, and high-temperature peak at 673–723 K and low-temperature peak at 473–573 K were utilized to quantify the strong and weak BAS, respectively.

investigated. In all reactions, only monobenzilation products and DBE could be detected by GC analysis. The conversion of benzyl alcohol at 353 K as a function of time is shown in Fig. 8, and the reaction results are summarized in Table 3.

3.3.1. Effect of the acidity of the H β zeolites

In the benzilation of BA with benzene or substituted benzene, the direct benzilation of aromatics with benzyl alcohol to yield monobenzilation products (1) competes with a two-step reaction mechanism that the condensation between benzyl alcohols to generate DBE (2), which can be further converted into the monobenzilation product with aromatic addition (3) (see Scheme 1). The direct benzilation of aromatics of pathway (1) is initiated by polarizing BA to generate benzyl cations as an electrophile, followed by an electrophilic addition to the aromatic ring [11]. A higher acid strength facilitates the formation of benzyl cations as electrophile, which promotes the reaction [34]. With similar textural properties, Micro-H β -2, having a higher acid strength of the BAS, causes a higher BA conversions with all arenes compared with Micro-H β -1 having a higher BAS density, as shown in Fig. 8. Moreover, the selectivities to the monobenzilation products of benzene and

toluene increased when using Micro-H β -2, but less effect when using *p*-xylene and mesitylene occurred in comparison with Micro-H β -1 as shown in Table 3. These observations have been attributed to the higher acid strength of Micro-H β -2, which can promote the formation of benzyl cations and the activation of less active arenes (benzene and toluene) for benzilation reaction. Similar trends were also observed with Meso-H β zeolites. However, Micro-H β zeolites cause higher conversions when using small arenes (benzene, toluene) than Meso-H β zeolites, but lower conversions when using arenes having large size (*p*-xylene, mesitylene). This is due to the limitation of the mass transfer of large arenes inside the micropores and will be discussed later.

3.3.2. Effect of nucleophilicity/proton affinity (PA)

Alkyl groups as nucleophilic reagents are electron donating substituents when bonded to aromatic rings. As shown in Table 4, the nucleophilicity and PA of aromatic rings increase with more substituted methyl groups on the aromatic ring. In the Friedel–Crafts reactions, more alkyl substituents on aromatic rings can donate more electrons to enhance the stability of electron-deficient carbocations. Therefore, increasing the nucleophilicity (more alkyl

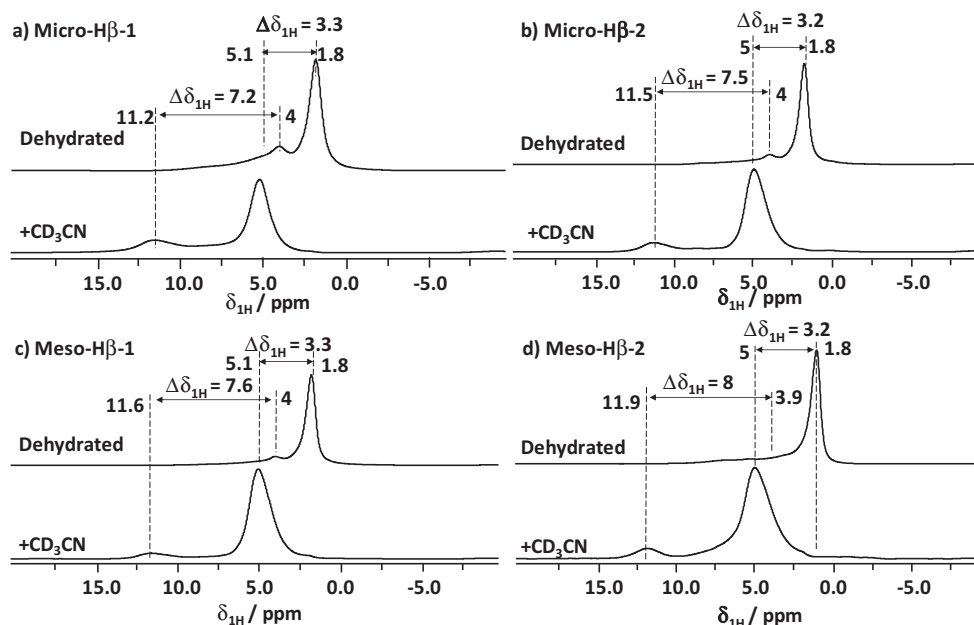


Fig. 6. ^1H MAS NMR spectra of the dehydrated H β zeolites recorded before (top) and after (bottom) adsorption of CD_3CN at room temperature and purged under a N_2 flow of 50 mL for 10 min.

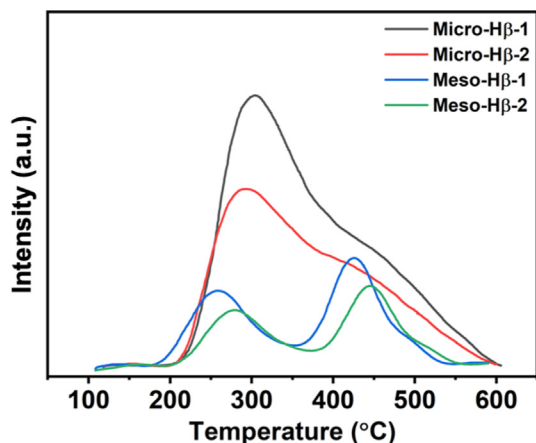


Fig. 7. NH_3 -TPD profiles of Micro-H β -1, Micro-H β -2, Meso-H β -1 and Meso-H β -2.

substituents) can facilitate the attack of benzylic cations on aromatic rings for electrophilic aromatic substitution reactions [6]. As expected, the conversion of BA (Table 5) and the yield of monobenylation products increased in the order of mesitylene > *p*-xylene > toluene over Meso-H β zeolites, except for benzene. However, the conversion of the benzylating agent (BA) was significantly decreased in the order of benzene > toluene > *p*-xylene > mesitylene, for both Micro-H β zeolites. This dependence of the catalytic activity on the nucleophilicity and PA of arenes has also been reported for mesoporous [Al]SBA-15 (pore size of 9.7–11.2 nm) in the benzylation of benzyl chloride with arenes, which is attributed to a stronger adsorption of arenes on active sites with a higher acid strength [53]. It should be noted that increasing the nucleophilicity of arenes by more substituted methyl groups can significantly increase the size of reactant/products as shown in Table 4. Since Meso-H β zeolites, which have similar or higher acid strength than Micro-H β zeolites, the low activity with using large arenes over Micro-H β zeolites is attributed to the constraint of the micropore size in this work, which hinders the

diffusion/access of large molecules to surface active sites by shape selectivity, such as mesitylene.

3.3.3. Effect of porosity of zeolites

As shown in Table 4, the molecular size of arenes (0.5–0.8), BA (0.7 nm), all monobenylation products (0.9–1 nm) and DBE (1.2 nm), is comparable to or even larger than the pore sizes of Micro-H β zeolites (1.1–1.2 nm), however, far smaller than the mesopores in Meso-H β zeolites (13.5–15.7 nm). Therefore, benzene and toluene reacted with BA in both micropores and mesopores; however, the conversion of *p*-xylene and mesitylene is favoured in mesopores due to the diffusion limitation of micropores. This results in the significant difference in catalytic activity as shown in Table 5. Since the porous structure has less effect on the diffusion/access of small arenes (benzene and toluene), Micro-H β zeolites with higher BAS density can promote the benzylation with BA via pathway (1) in Scheme 1, leading to 1.5 times higher BA conversion than over Meso-H β zeolites. However, when the arenes having large molecular size (*p*-xylene and mesitylene) were applied, Meso-H β zeolites exhibited a much higher activity than Micro-H β zeolites, providing an up to 2 times higher BA conversion.

The above-mentioned catalytic results have been further revealed by investigating the turnover frequency (TOF) of the benzylation reaction over H β zeolites. TOF is often employed to evaluate the performance of per active site on the catalyst surface during a reaction under study. The TOFs were determined at the initial reaction time (10 min). As shown in Fig. 9, these measurements revealed that the surface sites on Meso-H β zeolites are more active than those on Micro-H β zeolites for all arenes, not only for large reactants. The high BA conversion obtained with small arenes over Micro-H β zeolites is attributed to their high BAS density, compared to Meso-H β zeolites. It is obvious that the TOFs obtained for Micro-H β zeolites significantly decrease with increasing the molecular size of arenes, which was not observed for Meso-H β zeolites. This finding demonstrates the accessibility of BAS for reactants and products was dramatically improved inside mesopores, while diffusion/access limitations occur for large molecules in micropores. In theory, the TOF should increase with increasing the

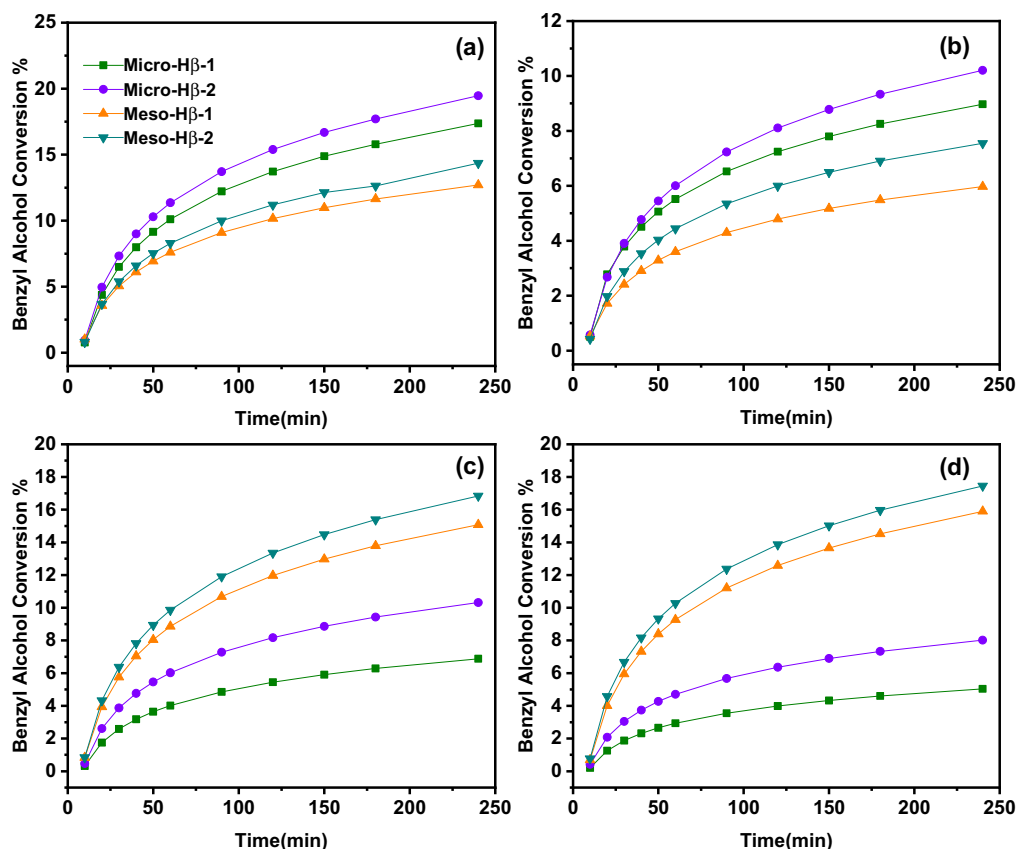


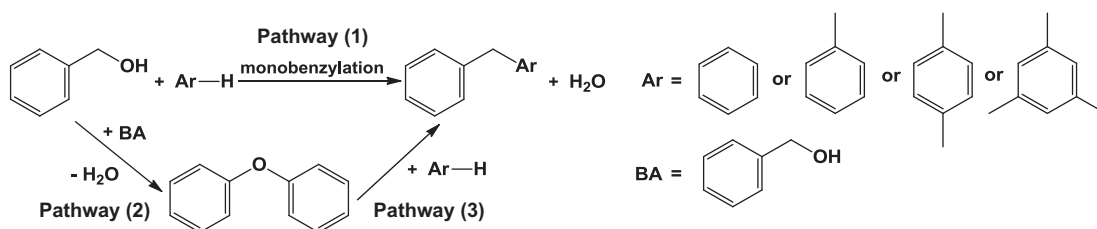
Fig. 8. Benzyl alcohol conversion in the alkylation of arenes with different catalysts: (a) benzene, (b) toluene, (c) p-xylene, and (d) mesitylene. Conditions: 25 mg catalysts, 3.5 mL arenes, 0.25 mL benzyl alcohol, reaction temperature of 353 K.

Table 3

Yield and selectivity in the benzylation of benzyl alcohol with arenes over H β zeolites.^a


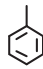
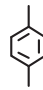
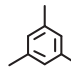
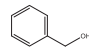
Arenes	Products	Yield % (Selectivity %)			
		Micro-H β -1	Micro-H β -2	Meso-H β -1	Meso-H β -2
		15.6 (89.7)	19.1 (98.2)	9.4 (74.0)	12.7 (88.6)
		7.7 (85.5)	8.9 (87.6)	3.8 (63.7)	6.1 (80.6)
		0.8 (8.8)	0.9 (9.1)	0.4 (6.1)	0.7 (8.7)
		5.2 (76.0)	7.8 (75.5)	13.5 (89.8)	14.9 (96.5)
		4.6 (90.7)	7.5 (93.5)	15.2 (95.4)	15.9 (97.1)

^a Conditions: 25 mg catalysts, 3.5 mL arenes, 0.25 mL benzyl alcohol, reacted at 353 K for 4 h. DPM, BMB, BDB and BTB are for diphenylmethane, benzyl-methylbenzene, 2-benzyl-1,4-dimethylbenzene and 2-benzyl-1,3,5-trimethylbenzene.



Scheme 1. Reaction pathway of arenes with benzyl alcohol.

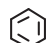
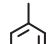
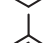

Table 4
Nucleophilicity and PA values of arenes, and molecular diameters of arenes and products.

Arènes					
Nucleophilicity ^a	−4.38	−3.94	−3.39	−2.82	
PA Value (kJ/mol)	750.2	784.1	794.5	836.4	
Molecular diameter of arenes (nm) ^b	0.5	0.54	0.67	0.8	0.7
Molecular diameter of products (nm) ^b	0.9	0.94/1.0	0.94	1.0	1.2

^a Nucleophilicity parameter as acquired from Mayr's equation, $\log(k) = S(N + E)$, in which E (Electrophilicity parameter) of An_2CH^+ was defined as 0 and S (nucleophile-specific slope parameter) of 2-methyl-1-pentene was defined as 1.

^b The molecular diameters of arenes are derived from refs. [54–56], and the size of BA and products are obtained from Chem 3D.

Table 5
BA conversion over H β catalysts in the benzylation of arenes.

	Micro-H β -1	Micro-H β -2	Meso-H β -1	Meso-H β -2
	17.4	19.5	12.7	14.4
	9	10.3	6.0	7.5
	6.9	10.2	15.1	15.5
	5.0	8.0	15.9	16.4

^a Conditions: 25 mg catalysts, 0.25 mL benzyl alcohol in 3.5 mL arenes, reacted at 353 K for 4 h.

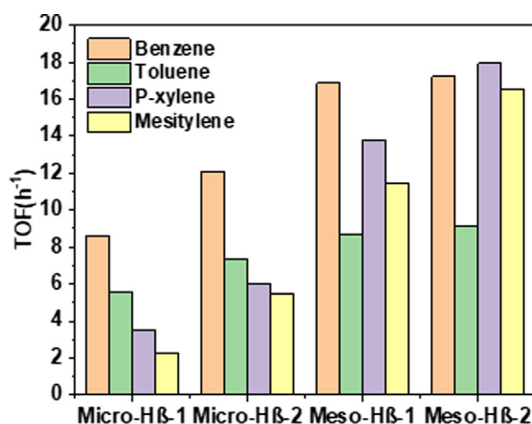


Fig. 9. Turnover frequencies (TOF) of BA in the benzylation with different arenes over various H β zeolites. Conditions: 25 mg catalysts, 3.5 mL arenes, 0.25 mL benzyl alcohol, reacted at 353 K for 10 min.

nucleophilicity of arenes under the same conditions without the shape selectivity of zeolite pore size. However, a similar or slight decrease of TOF values was observed for Meso-H β zeolites. This behaviour could be caused by a molecular size similar to the distance between two active sites, indicated by the number of BAS per nm² in Table 2. As an example, the average distance between two sites on the Meso-H β -1 zeolite is close to the molecular size of *p*-xylene, mesitylene and BA, and thus, the reaction at one site and the benzylation product with a larger size could inhibit the reaction at neighbouring sites.

In the following, the shape-selectivity effect of zeolites on the selectivity/yield of desired products has been considered. Compared to Micro-H β zeolites, a high DBE selectivity was obtained in the conversion of benzene and toluene over Meso-H β zeolites. This indicates that the mass transfer can be strongly enhanced in

mesopores to facilitate the formation of DBE, but is hindered in the micropores via shape selectivity. The conversion of DBE with arenes is inhibited by the rate limiting step in pathway (3) in Scheme 1. This is in agreement with previous studies [35,57], that BA is more favourable to proceed by self-condensation, rather than the direct benzylation with arenes having low nucleophilicity. As observed by Chiu et al. [35] for the benzylation of toluene with BA at 383 K, the rate constant k in the conversion of BA to DBE (pathway (2) in Scheme 1) are $3 \times 10^{-3} \text{ s}^{-1}$ and $3.5 \times 10^{-3} \text{ s}^{-1}$ for microporous H-Beta (Si/Al = 75, pore size of 0.56 nm) and mesoporous SBA-15 (Si/Al = 70, pore size of 5.2 nm), respectively. The rate constant k in the conversion of DBE to benzyl-methylbenzene (BMB) (pathway (3) in Scheme 1) are $1.5 \times 10^{-5} \text{ s}^{-1}$ and $9.0 \times 10^{-4} \text{ s}^{-1}$ for microporous H-Beta and mesoporous SBA-15, respectively. Obviously, increasing the pore size can promote the formation of DBE with BA even with much lower Brønsted acidity on SBA-15, however, the conversion of DBE to BMB is limited. Therefore, Micro-H β zeolites provided a higher selectivity to DPM and BMB than Meso-H β zeolites. With increasing the molecular size of arenes, the nucleophilicity of arenes is increased, which can promote their reaction with BA over the formation of DBE, and thus, enhances the selectivity (>95%) to BDB and BTB over Meso-H β zeolites. Over Micro-H β zeolites, even a small DBE selectivity (<10%) was still achieved with high selectivities to BDB and BTB. The yields of BDB and BTB are only a quarter to half of those obtained with Meso-H β zeolites, due to the limitation of mass transfer. The yields of monobenzylation products increased in the order of BMB < BDB < BTB over Meso-H β zeolites, which is in line with the nucleophilicity of arenes, similar to those reported for homogeneous catalysts [6]. This indicates that the presence of mesopores can remarkably enhance the catalytic performance of H β zeolites in the benzylation of large arenes.

In the literature [29,58], benzylation of benzene is often carried out at its boiling point of 353 K. In the benzylation of toluene, *p*-xylene, and mesitylene, 373–383 K is the frequently applied reaction temperature, which is the boiling point of toluene [16,34,35]. Therefore, benzylation with arenes, except benzene, was further carried out at 383 K to confirm above observations. The conversion of BA is significantly enhanced as shown in Fig. 10. All catalysts retained their high selectivity to the monobenzylation products (Table 6) as obtained at 353 K. Micro-H β zeolites provide higher BA conversion with using toluene, while Meso-H β zeolites are more active with using *p*-xylene and mesitylene. For example, in the benzylation of mesitylene, the conversion of BA was significantly enhanced from ca. 16% at 353 K to ca. 95% at 383 K over Meso-H β zeolites, while only increased from 5 to 8% to 40% over Micro-H β zeolites. Moreover, the yield obtained with Meso-H β zeolites is almost 2–4 times higher than that obtained with Micro-H β zeolites. This is similar as those observed above that the small pore size of Micro-H β zeolites constrains the mass transfer of large arenes/products by shape selectivity. The TOF values obtained at 383 K are remarkably enhanced with temperature

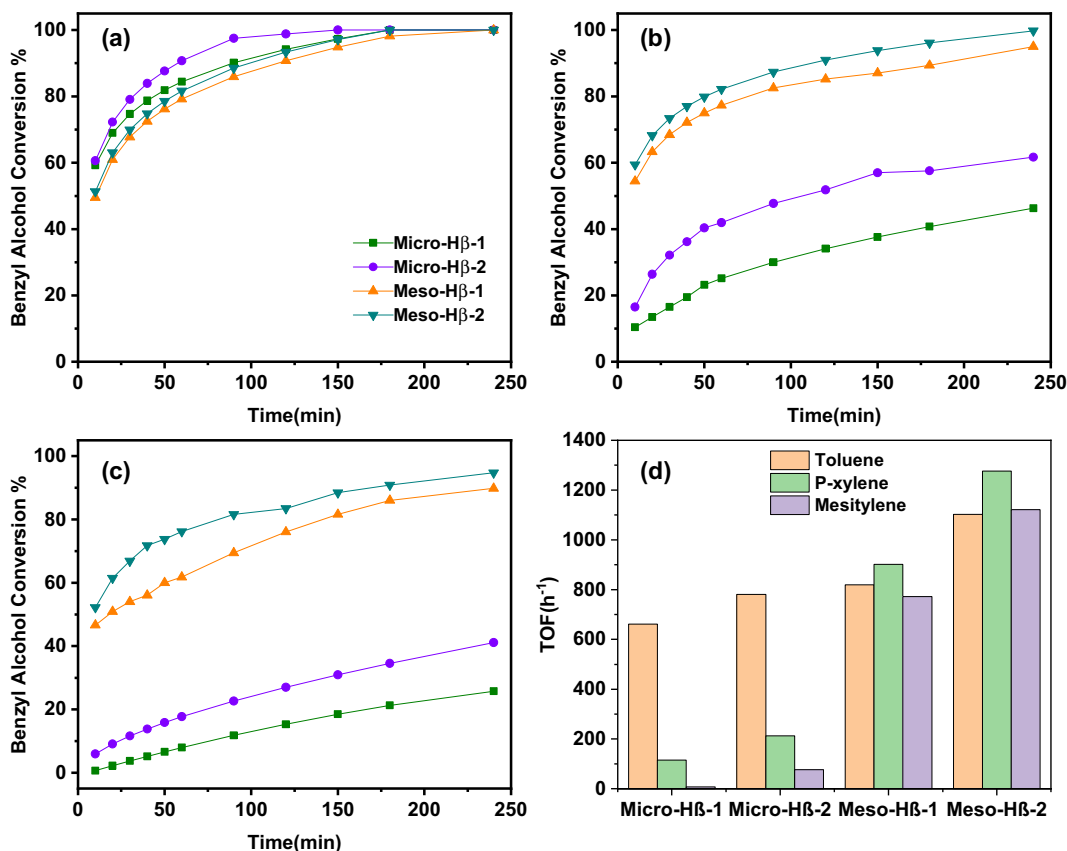
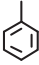
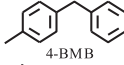
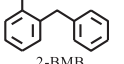
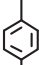
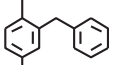
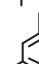
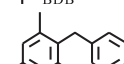


Fig. 10. Benzyl alcohol conversion in the benzylation of toluene (a), p-xylene (b), and mesitylene (c) and the TOF of BA in the benzylation with arenes for different catalysts (d). Conditions: 25 mg catalysts, 3.5 mL mesitylene, 0.25 mL benzyl alcohol, reaction temperature of 383 K.

Table 6

Yield and selectivity in the benzylation of benzyl alcohol with arenes over H β zeolites.^a

Arenes	Products	Yield % (Selectivity %)			
		Micro-H β -1	Micro-H β -2	Meso-H β -1	Meso-H β -2
	 4-BMB	80.4 (80.4)	79.9 (79.9)	62.7 (62.7)	81.6 (81.6)
	 2-BMB	8.4 (8.4)	9.5 (9.5)	6.0 (6.0)	7.7 (7.7)
	 BDB	31.3 (67.6)	46.8 (76.0)	66.3 (69.7)	79.4 (79.4)
	 BTB	15.2 (59)	26.5 (64.5)	62.3 (69.4)	69.2 (73.1)

^a Conditions: 25 mg catalysts, 3.5 mL arenes, 0.25 mL benzyl alcohol, reacted at 383 K for 4 h.

compared to those obtained at 353 K. The TOF values obtained with the Meso-H β -2 zeolite significantly increased for 140 times using toluene, while increased from 70 times using mesitylene. This indicates that the temperature would have a significant effect on the mass transfer of low reactive arenes at their boiling point, such as for benzene and toluene. As observed in Fig. 9, the TOF values obtained with Meso-H β zeolites are slightly change with using different arenes, while those obtained Micro-H β zeolites are significantly reduced with increasing the molecular size of arenes. These observations clearly demonstrate that the shape selectivity by porosity of zeolites has strong effect on their activity.

Obviously, mesopores in H β zeolites can significantly enhanced the activity of these catalysts due to the improved mass transfer and the large pore size facilitates the formation of BTB, compared to micropores. This is in an agreement with the observations of Jin et al. [57] and Liu et al. [16] in the comparison of Micro-H-ZSM-5 and Meso-H-ZSM-5 zeolites. In the benzylation of benzene with BA, Wang et al. [58] have shown that Meso-ZSM-5 is more active in the conversion of BA than Micro-ZSM-5 (71% for Meso-ZSM-5 vs. 11% for ZSM-5) at 353 K for 6 h. Chiu et al. [35] reported that the application of mesoporous SBA-15 for the benzylation of toluene to BMB provides a two times higher of reaction rate k than using microporous H β zeolites ($1.5 \times 10^{-3} \text{ s}^{-1}$ vs. $8.0 \times 10^{-4} \text{ s}^{-1}$),

even the latter has much higher Brønsted acidity. Recently, mesoporous H β zeolites has been employed in the benzylation of naphthalene with benzyl chloride, where the catalytic performance was remarkably enhanced by improving the diffusion of reactant/products and the accessibility of surface sites by introducing mesopores. In terms of the catalytic performance of H β zeolites in this work, it demonstrates that suitable porosity of zeolites is crucial for both a high conversion of BA and a high shape selectivity to monobenzylation products in the benzylation of arenes.

4. Conclusion

In this study, H β zeolites with different Si/Al ratios and pore sizes (micropore and mesopore) were successfully prepared. The mesopores (13–15 nm) and micropores (1.1 nm) of H β zeolites were confirmed by XRD and BET and TEM techniques. The local structure and acidity of H β zeolites were studied by solid-state NMR spectroscopy. Mainly BAS could be detected on H β zeolites and quantified by ^1H MAS NMR experiments. The acidity characterization showed that Micro-H β zeolites exhibit a higher BAS density but a slightly lower strength than Meso-H β zeolites.

The obtained H β zeolites were applied in the conversion of benzyl alcohol (BA) with various arenes to investigate the effect of Brønsted acidity, reactant nucleophilicity and shape selectivity on benzylation reactions. Increasing the Brønsted acid strength can promote benzylation reaction over Micro-H β and Meso-H β zeolites. Micro-H β zeolites are more active and selective in the benzylation of benzene and toluene, but less active in the conversion of *p*-xylene and mesitylene (Fig. 8). Compared to small arenes, bulk arenes with more alkyl groups having a higher nucleophilicity are more active in electrophilic aromatic substitution reaction. The low activity of bulk arenes in benzylation reactions has been attributed to the shape selectivity of micropores, which limits the diffusion of bulk arenes to active sites. These mass transport limitations have been significantly improved by introducing mesopores in H β zeolites, confirmed by the TOF shown in Fig. 9, particularly for bulk arenes (xylene and mesitylene). Therefore, Meso-H β zeolites are much more active than Micro-H β zeolites in the conversion of bulky arenes. For example, when mesitylene was applied, Meso-H β zeolites provide a ca. 2 times higher conversion of BA and a 2–4 times higher yield of BTB than obtained with Micro-H β zeolites. Therefore, this work demonstrates that introducing mesopores with suitable acidity in H β zeolites are keys for tailoring a high catalytic performance in the benzylation of arenes with benzyl alcohol.

Notes

The authors declare no competing financial interest.

Author contributions

The manuscript was written through contributions of all authors. All authors have given approval to the final version of the manuscript.

Acknowledgment

This work was supported by the Australian Research Council Discovery Projects (DP150103842) and Discovery Earlier Career Research Project (DE190101618), the SOAR Fellowship, and the Sydney Nano Grand Challenge from the University of Sydney from the University of Sydney.

References

- [1] L.T. Mika, E. Csefalvay, A. Nemeth, Catalytic conversion of carbohydrates to initial platform chemicals: Chemistry and Sustainability, *Chem. Rev.* 118 (2018) 505–613.
- [2] G.W. Huber, S. Iborra, A. Corma, Synthesis of transportation fuels from biomass: Chemistry, catalysts, and engineering, *Chem. Rev.* 106 (2006) 4044–4098.
- [3] Z. Sun, G. Bottari, A. Afanasenko, M.C.A. Stuart, P.J. Deuss, B. Fridrich, K. Barta, Complete lignocellulose conversion with integrated catalyst recycling yielding valuable aromatics and fuels, *Nat. Catal.* 1 (2018) 82–92.
- [4] H. Wu, J. Song, C. Xie, C. Wu, C. Chen, B. Han, Efficient and mild transfer hydrogenolytic cleavage of aromatic ether bonds in lignin-derived compounds over Ru/C, *ACS Sustain. Chem. Eng.* 6 (2018) 2872–2877.
- [5] M. Wang, X. Zhang, H. Li, J. Lu, M. Liu, F. Wang, Carbon modification of nickel catalyst for depolymerization of oxidized lignin to aromatics, *ACS Catal.* 8 (2018) 1614–1620.
- [6] G.A. Olah, *Friedel-Crafts chemistry*, Wiley-Interscience, New York, 1973.
- [7] V.D. Chaube, Benzylation of benzene to diphenylmethane using zeolite catalysts, *Catal. Commun.* 5 (2004) 321–326.
- [8] V. Prakash Reddy, G.K. Surya Prakash, Friedel-Crafts reactions, in: Kirk-Othmer (Ed.), *Kirk-Othmer Encyclopedia of Chemical Technology*, Wiley, Hoboken, NJ, 2013.
- [9] A.P. Bolton, *Zeolite chemistry and catalysis*, Am. Chem. Soc., Washington DC, 1976.
- [10] Y. Li, L. Li, J.H. Yu, Applications of zeolites in sustainable chemistry, *Chem* 3 (2017) 928–949.
- [11] B. Coq, V. Gourves, F. Figueras, Benzylation of toluene by benzyl-chloride over protonic zeolites, *Appl. Catal. A-Gen.* 100 (1993) 69–75.
- [12] A.P. Singh, B. Jacob, S. Sugunan, Liquid-phase selective benzylation of *o*-xylene using zeolite catalysts, *Appl. Catal. A-Gen.* 174 (1998) 51–60.
- [13] N. Candu, M. Florea, S.M. Coman, V.I. Parvulescu, Benzylation of benzene with benzyl alcohol on zeolite catalysts, *Appl. Catal. A-Gen.* 393 (2011) 206–214.
- [14] M. Salavati-Niasari, J. Hasanalian, H. Najafian, Alumina-supported FeCl $_3$, MnCl $_2$, CoCl $_2$, NiCl $_2$, and ZnCl $_2$ as catalysts for the benzylation of benzene by benzyl chloride, *J. Mol. Catal. A-Chem.* 209 (2004) 209–214.
- [15] Y. Izumi, M. Ogawa, K. Urabe, Alkali-metal salts and ammonium-salts of kegglin-type heteropolyacids as solid acid catalysts for liquid-phase Friedel-Crafts reactions, *Appl. Catal. A-Gen.* 132 (1995) 127–140.
- [16] B. Liu, Z. Chen, J. Huang, H. Chen, Y. Fang, Direct synthesis of hierarchically structured MFI zeolite nanosheet assemblies with tailored activity in benzylation reaction, *Micropor. Mesopor. Mater.* 273 (2019) 235–242.
- [17] Y. He, Q. Zhang, X. Zhan, D. Cheng, F. Chen, Aluminum impregnated silica catalyst for Friedel-Crafts reaction: Influence of ordering mesostructure, *Chin. J. Chem. Eng.* 25 (2017) 1533–1538.
- [18] S.K. Saxena, N. Viswanadham, Enhanced catalytic properties of mesoporous mordenite for benzylation of benzene with benzyl alcohol, *Appl. Surf. Sci.* 392 (2017) 384–390.
- [19] Y. Wang, J. Ma, F. Ren, J. Du, R. Li, Hierarchical architectures of ZSM-5 nanocrystalline aggregates with particular catalysis for larger molecule reaction, *Micropor. Mesopor. Mater.* 240 (2017) 22–30.
- [20] W. Hao, W. Zhang, Z. Guo, J. Ma, R. Li, Mesoporous Beta zeolite catalysts for benzylation of naphthalene: Effect of pore structure and acidity, *Catal.* 8 (2018) 504.
- [21] V.R. Choudhary, S.K. Jana, B.P. Kiran, Alkylation of benzene by benzyl chloride over H-ZSM-5 zeolite with its framework Al completely or partially substituted by Fe or Ga, *Catal. Letters* 59 (1999) 217–219.
- [22] S.N. Jun, R. Ryoo, Aluminum impregnation into mesoporous silica molecular sieves for catalytic application to Friedel-Crafts alkylation, *J. Catal.* 195 (2000) 237–243.
- [23] F. Wang, W. Ueda, High catalytic efficiency of nanostructured molybdenum trioxide in the benzylation of arenes and an investigation of the reaction mechanism, *Chem. A Euro. J.* 15 (2009) 742–753.
- [24] N. Narendar, K.V.V.K. Mohan, S.J. Kulkarni, I.A.K. Reddy, Liquid phase benzylation of benzene and toluene with benzyl alcohol over modified zeolites, *Catal. Commun.* 7 (2006) 583–588.
- [25] K. Bachari, A. Touileb, O. Cherifi, Catalytic properties of antimony-SBA-15 materials in the benzylation of aromatics reactions, *Kinetics Catal.* 50 (2009) 407–413.
- [26] V.R. Choudhary, S.K. Jana, B.P. Kiran, Highly active Si-MCM-41-Supported Ga $_2$ O $_3$ and In $_2$ O $_3$ catalysts for Friedel-Crafts-type benzylation and acylation reactions in the presence or absence of moisture, *J. Catal.* 192 (2000) 257–261.
- [27] V.R. Choudhary, S.K. Jana, Benzylation of benzene by benzyl chloride over Fe-, Zn-, Ga- and In-modified ZSM-5 type zeolite catalysts, *Appl. Catal. A-Gen.* 224 (2002) 51–62.
- [28] Y.Y. Sun, S. Walspurger, J.P. Tessonnier, B. Louis, J. Sommer, Highly dispersed iron oxide nanoclusters supported on ordered mesoporous SBA-15: A very active catalyst for Friedel-Crafts alkylations, *Appl. Catal. A-Gen.* 300 (2006) 1–7.
- [29] S.N. Koyande, R.G. Jaiswal, R.V. Jayaram, Reaction kinetics of benzylation of benzene with benzyl chloride on sulfate-treated metal oxide catalysts, *Ind. Eng. Chem. Res.* 37 (1998) 908–913.
- [30] S. Li, H. Zhou, C.H. Jin, N.D. Feng, F. Liu, F. Deng, J.Q. Wang, W. Huang, L.P. Xiao, J. Fan, Formation of subnanometer Zr-WO $_x$ clusters within mesoporous W-Zr mixed oxides as strong solid acid catalysts for Friedel-Crafts alkylation, *J. Phys. Chem. C* 118 (2014) 6283–6290.

- [31] G. Kamalakar, K. Komura, Y. Kubota, Y. Sugi, Friedel-Crafts benzylation of aromatics with benzyl alcohols catalyzed by heteropoly acids supported on mesoporous silica, *J. Chem. Technol. Biot.* 81 (2006) 981–988.
- [32] X. Li, R. Prins, J.A. van Bokhoven, Synthesis and characterization of mesoporous mordenite, *J. Catal.* 262 (2009) 257–265.
- [33] J.C. Groen, T. Sano, J.A. Moulijn, J. Pérez-Ramírez, Alkaline-mediated mesoporous mordenite zeolites for acid-catalyzed conversions, *J. Catal.* 251 (2007) 21–27.
- [34] Z.C. Wang, L. Wang, Z. Zhou, Y.Y. Zhang, H.T. Li, C. Stampfl, C.H. Liang, J. Huang, Benzylation of arenes with benzyl chloride over H-Beta zeolite: Effects from acidity and shape-selectivity, *J. Phys. Chem. C* 121 (2017) 15248–15255.
- [35] J.J. Chiu, D.J. Pine, S.T. Bishop, B.F. Chmelka, Friedel-Crafts alkylation properties of aluminosilica SBA-15 meso/macroporous monoliths and mesoporous powders, *J. Catal.* 221 (2004) 400–412.
- [36] K. Möller, B. Yilmaz, R.M. Jacubinas, U. Müller, T. Bein, One-step synthesis of hierarchical zeolite Beta via network formation of uniform nanocrystals, *J. Am. Chem. Soc.* 133 (2011) 5284–5295.
- [37] Z. Wang, L. Wang, Y. Jiang, M. Hunger, J. Huang, Cooperativity of Brønsted and Lewis acid sites on zeolite for glycerol dehydration, *ACS Catal.* 4 (2014) 1144–1147.
- [38] J. Stelzer, M. Paulus, M. Hunger, J. Weitkamp, Hydrophobic properties of all-silica zeolite beta. Dedicated to Professor Lovat V.C. Rees in recognition and appreciation of his lifelong devotion to zeolite science and his outstanding achievements in this field, *Micropor. Mesopor. Mater.* 22 (1998) 1–8.
- [39] M. Thommes, K. Kaneko, A.V. Neimark, J.P. Olivier, F. Rodriguez-Reinoso, J. Rouquerol, K.S.W. Sing, Physisorption of gases, with special reference to the evaluation of surface area and pore size distribution (IUPAC Technical Report), *Pure Appl. Chem.* 87 (2015) 1051–1069.
- [40] C.B. Dartt, M.E. Davis, Chapter 6 Applications of zeolites to fine chemicals synthesis, *Catal. Today* 19 (1994) 151–186.
- [41] M. Hunger, Solid-state NMR spectroscopy, in: A.W. Chester, E.G. Derouane (Eds.), *Zeolite Characterization and Catalysis - A Tutorial*, Springer, Netherlands, 2010.
- [42] Y. Jiang, J. Huang, W. Dai, M. Hunger, Solid-state nuclear magnetic resonance investigations of the nature, property, and activity of acid sites on solid catalysts, *Solid State Nucl. Magn. Reson.* 39 (2011) 116–141.
- [43] J. Huang, Y. Jiang, V.R.R. Marthala, B. Thomas, E. Romanova, M. Hunger, Characterization and acidic properties of aluminum-exchanged zeolites X and Y, *J. Phys. Chem. C* 112 (2008) 3811–3818.
- [44] G. Bellussi, G. Pazzuconi, C. Perego, G. Girotti, G. Terzoni, Liquid-phase alkylation of benzene with light olefins catalyzed by beta-zeolites, *J. Catal.* 157 (1995) 227–234.
- [45] K. Leng, Y. Wang, C. Hou, C. Lancelot, C. Lamonier, A. Rives, Y. Sun, Enhancement of catalytic performance in the benzylation of benzene with benzyl alcohol over hierarchical mordenite, *J. Catal.* 306 (2013) 100–108.
- [46] J. Huang, N. van Vegten, Y. Jiang, M. Hunger, A. Baiker, Increasing the Brønsted Acidity of flame-derived silica/alumina up to zeolitic strength, *Angew. Chem. Int. Ed.* 49 (2010) 7776–7781.
- [47] Z.C. Wang, Y.J. Jiang, O. Lafon, J. Trebosc, K.D. Kim, C. Stampfl, A. Baiker, J.P. Amoureux, J. Huang, Brønsted acid sites based on penta-coordinated aluminum species, *Nat. Commun.* 7 (2016) 13820.
- [48] F. Deng, Y. Yue, C.H. Ye, Observation of nonframework Al species in zeolite beta by solid-state NMR spectroscopy, *J. Phys. Chem. B* 102 (1998) 5252–5256.
- [49] W.J. Mortier, Zeolite electronegativity related to physicochemical properties, *J. Catal.* 55 (1978) 138–145.
- [50] A.A. Gabrienko, I.G. Danilova, S.S. Arzumanov, A.V. Toktarev, D. Freude, A.G. Stepanov, Strong acidity of silanol groups of zeolite beta: Evidence from the studies by IR spectroscopy of adsorbed CO and H-1 MAS NMR, *Micropor. Mesopor. Mater.* 131 (2010) 210–216.
- [51] E. Brunner, K. Beck, M. Koch, L. Heeribout, H.G. Karge, Verification and quantitative-determination of a new-type of Brønsted acid sites in H-ZSM-5 by H-1 magic-angle-spinning nuclear-magnetic-resonance spectroscopy, *Micropor. Mater.* 3 (1995) 395–399.
- [52] L. Yang, Y. Aizhen, X. Qinhu, Acidity, diffusion and catalytic properties of the silicoaluminophosphate SAPO-11, *Appl. Catal.* 67 (1991) 169–177.
- [53] A. Vinu, D.P. Sawant, K. Ariga, M. Hartmann, S.B. Halligudi, Benzylation of benzene and other aromatics by benzyl chloride over mesoporous AISBA-15 catalysts, *Micropor. Mesopor. Mater.* 80 (2005) 195–203.
- [54] J.J. Vijaya, L.J. Kennedy, G. Sekaran, K.S. Nagaraja, Sol-gel derived (Sr, Ni)Al₂O₄ composites for benzene and toluene sensors, *Mater. Lett.* 61 (2007) 5213–5216.
- [55] S. Nakashima, Y. Takahashi, M. Kiguchi, Effect of the environment on the electrical conductance of the single benzene-1,4-diamine molecule junction, *Beilstein J. Nanotech.* 2 (2011) 755–759.
- [56] P.S. Bácia, D. Guimarães, P.A.P. Mendes, J.A.C. Silva, V. Guillerme, H. Chevreau, C. Serre, A.E. Rodrigues, Reverse shape selectivity in the adsorption of hexane and xylene isomers in MOF UiO-66, *Micropor. Mesopor. Mater.* 139 (2011) 67–73.
- [57] H. Jin, M.B. Ansari, E.-Y. Jeong, S.E. Park, Effect of mesoporosity on selective benzylation of aromatics with benzyl alcohol over mesoporous ZSM-5, *J. Catal.* 291 (2012) 55–62.
- [58] Y. Wang, J. Song, N.C. Baxter, G.T. Kuo, S. Wang, Synthesis of hierarchical ZSM-5 zeolites by solid-state crystallization and their catalytic properties, *J. Catal.* 349 (2017) 53–65.